BJR

KNEE

Metal-backed *versus* all-polyethylene unicompartmental knee arthroplasty

PROXIMAL TIBIAL STRAIN IN AN EXPERIMENTALLY VALIDATED FINITE ELEMENT MODEL

C. E. H. Scott,
M. J. Eaton,
R. W. Nutton,
F. A. Wade,
S. L. Evans,
P. Pankaj

University of Edinburgh, Edinburgh, United Kingdom

■ C. E. H. Scott, MSc, FRCS(Tr&Orth), MD, Knee Research Fellow, School of Engineering, University of Edinburgh, Alexander Graham Bell Building, Mayfield Road, Edinburgh EH9 3JL, UK.
■ P. Pankaj, PhD, Reader in Numerical Modelling, School of Engineering, University of Edinburgh, Alexander Graham Bell Building, Mayfield Road, Edinburgh EH9 3JL, UK.
■ M. J. Eaton, BEng, PhD, Research Associate,
■ S. L. Evans, BEng, PhD, Professor of Engineering, Cardiff School of Engineering, Cardiff University Institute of Mechanical and Manufacturing Engineering, Queen's Buildings, The Parade, Cardiff CF24 3AA, UK.
■ R. W. Nutton, MD, FRCS(Orth), Consultant Orthopaedic Surgeon,
■ F. A. Wade, FRCSEd(Orth), Consultant Orthopaedic Surgeon, Department of Orthopaedics, Royal Infirmary of Edinburgh, 51 Little France Crescent, Old Dalkeith Road, Edinburgh EH16 4SA, UK.

Correspondence should be sent to C. E. H. Scott at chloe.scott@nhslothian.scot.nhs.uk

doi: 10.1302/2046-3758.61.BJR-2016-0142.R1

Bone Joint Res 2017;6:22–30.

Received: 31 May 2015;
Accepted: 20 September 2016

Objectives

Up to 40% of unicompartmental knee arthroplasty (UKA) revisions are performed for unexplained pain which may be caused by elevated proximal tibial bone strain. This study investigates the effect of tibial component metal backing and polyethylene thickness on bone strain in a cemented fixed-bearing medial UKA using a finite element model (FEM) validated experimentally by digital image correlation (DIC) and acoustic emission (AE).

Materials and Methods

A total of ten composite tibias implanted with all-polyethylene (AP) and metal-backed (MB) tibial components were loaded to 2500 N. Cortical strain was measured using DIC and cancellous microdamage using AE. FEMs were created and validated and polyethylene thickness varied from 6 mm to 10 mm. The volume of cancellous bone exposed to $<$ -3000 με (pathological loading) and $<$ -7000 με (yield point) minimum principal (compressive) microstrain and $>$ 3000 με and $>$ 7000 με maximum principal (tensile) microstrain was computed.

Results

Experimental AE data and the FEM volume of cancellous bone with compressive strain $<$ -3000 με correlated strongly: $R = 0.947$, $R^2 = 0.847$, percentage error 12.5% ($p < 0.001$). DIC and FEM data correlated: $R = 0.838$, $R^2 = 0.702$, percentage error 4.5% ($p < 0.001$). FEM strain patterns included MB lateral edge concentrations; AP concentrations at keel, peg and at the region of load application. Cancellous strains were higher in AP implants at all loads: 2.2- (10 mm) to 3.2-times (6 mm) the volume of cancellous bone compressively strained $<$ -7000 με.

Conclusion

AP tibial components display greater volumes of pathologically overstrained cancellous bone than MB implants of the same geometry. Increasing AP thickness does not overcome these pathological forces and comes at the cost of greater bone resection.

Cite this article: *Bone Joint Res* 2017;6:22–30.

Keywords: Unicompartmental knee arthroplasty, Bone strain, Finite element analysis

Article focus

- Experimental validation of a finite element model of medial unicompartmental knee arthroplasty (UKA) using acoustic emission data and digital image correlation.
- Investigation of the effect of UKA implant thickness and metal backing on cancellous bone strain.

Key messages

- All-polyethylene tibial components display greater proximal tibial cancellous bone strain than metal-backed implants of the same geometry at physiological loads.
- Altering all-polyethylene component thickness markedly affects proximal tibial strain with thinner implants associated with greater strains.

Strengths and limitations

- Strengths of this finite element study include experimental validation, the examination of bone strain and a novel investigation of metal backing in UKA.
- Limitations of this study include the use of composite tibias, the performance of a linearly elastic analysis and the lack of kinematic analysis.

Introduction

The ten-year survival of unicompartmental knee arthroplasty (UKA) varies from 80% to 96% between implants and institutions.[1-3] Unexplained pain is a leading cause of UKA failure, accounting for 24% to 48% of revisions across registries.[1-3] Elevated proximal tibial strain and microdamage may cause this pain.[4,5] Joint registries do not distinguish between metal-backed (MB) and all-polyethylene (AP) UKAs and there is a paucity of biomechanical evidence to inform decisions between implants of different material.[6] Finite element models (FEMs) of UKAs are few in number and most frequently analyse mobile-bearing UKAs.[4,7-12] The effect of implant thickness on proximal tibial strain has not been reported.

Orthopaedic FEMs are typically validated using strain gauge experiments. These measure strain only over the surface area to which they are attached. Acoustic emission (AE) can measure failure initiated inside a solid by detecting sound waves produced as material undergoes post-elastic deformation from plasticity or damage.[13] During plasticity, dislocation movement and cracking releases elastic waves of energy detectable on the material's surface by piezoelectric sensors in real time.[13] AE-detected microdamage has been verified using micro-CT (μCT).[13] To our knowledge, AE has not previously been used to validate a FEM. Digital image correlation (DIC) is a non-destructive technique which measures surface strain. It involves observing with cameras the pattern of deformation on loading of a high-contrast speckle pattern applied to a surface. DIC has been used to measure macroscopic and microscopic surface strain in both cadaveric[14] and synthetic bone[15] and has been used previously to validate FEMs.[16,17]

The aims of this study were:

- the validation of a finite element model of the proximal tibia implanted with cemented fixed-bearing medial UKAs using experimental AE and DIC data;[15]
- to investigate the effect of UKA implant thickness and metal backing on cancellous bone strain.

We hypothesised that proximal tibial cancellous bone would experience greater strain under AP tibial components than MB implants and that this would be exacerbated in thinner implants.

Materials and Methods

Mechanical testing. Full details of the experimental methods can be found in the previous study.[15] A total of ten fourth-generation composite Sawbone tibias (model #3401, density Pcf(g/cc) 102 (1.64); Pacific Research Laboratories, Vashon, Washington) were implanted with Sigma Partial (DePuy, Johnson & Johnson Professional Inc, Raynham, Massachusetts) fixed-bearing, non-conforming cemented medial UKA tibial components: five AP, five MB. These synthetic bones are a composite of rigid polyurethane foam (Young's modulus E = 0.155 GPa) simulating cancellous bone and short fibre-filled epoxy composite (E = 16.7 GPa) simulating cortical bone. They have < 10% interspecimen variability and material properties, and mechanical behaviour similar to those of human cadaveric bone.[18] The geometry of third and fourth generation tibias is identical.

The proximal tibia was coated with matt white paint and a black speckle pattern applied. Then two charge-coupled DIC cameras (Limess, Messtechnik und Software GmbH, Krefeld, Germany) were positioned to view the anteromedial tibia. Implants were loaded using a servohydraulic machine (Losenhausen Maschinenbau, Düsseldorf, Germany) in 500 N increments to a 2500 N medial load. Cameras were calibrated and images taken at 500 N increments. Images were 60 mm wide, giving a resultion of 0.0375 mm/pixel. Strain in the vertical direction was measured at ⩾ 80 consecutive points along an anteromedial line. DIC analysis was performed using Istra 4D 3.1 software (Dantec Dynamics, Skovlunde, Denmark). AE was measured by two Pancom Pico-z piezoelectric AE sensors (125 kHz to 750 kHz; Pancom, Huntingdon, United Kingdom) and IL40S preamplifiers (Mistras Group Ltd, Princeton Junction, New Jersey). AE recording was continuous and activity > 45 dB amplitude registered as a 'hit'. Computer analysis was performed using AEWin 3.5 software (Physical Acoustics, Princeton Junction, New Jersey).

Finite element model creation and validation. A computer-aided design (CAD) model of a third-generation left composite tibia was obtained from the public domain[19] and imported into ABAQUS CAE Version 6.12 (Simulia, Dassault Systemes, Waltham, Massachusetts) as cortical and cancellous parts. Anatomical axes were defined in coronal and sagittal planes. The proximal tibia was cut perpendicular to the coronal anatomical axis at 6 mm depth with 6° of posterior slope. The tibia was cut distally at 200 mm below the intercondylar eminence to reduce computational effort.

CAD models of tibial components (size 3 MB tibia, 8 mm tibial insert and a size 3 8 mm AP tibia) and 1.5 mm cement mantles were created using Autodesk Inventor 2012 (Autodesk Inc., San Rafael, California) based on implant measurements taken with a digital calliper sensitive to 1/100 mm. These were imported into ABAQUS CAE Version 6.12 and assembled creating two models (Fig. 1):

- a composite tibia with a cemented 8 mm AP tibial component;
- a composite tibia with a cemented MB tibial component and 8 mm polyethylene insert.

All materials were assumed to be isotropic, homogenous and linearly elastic. Material properties are shown in

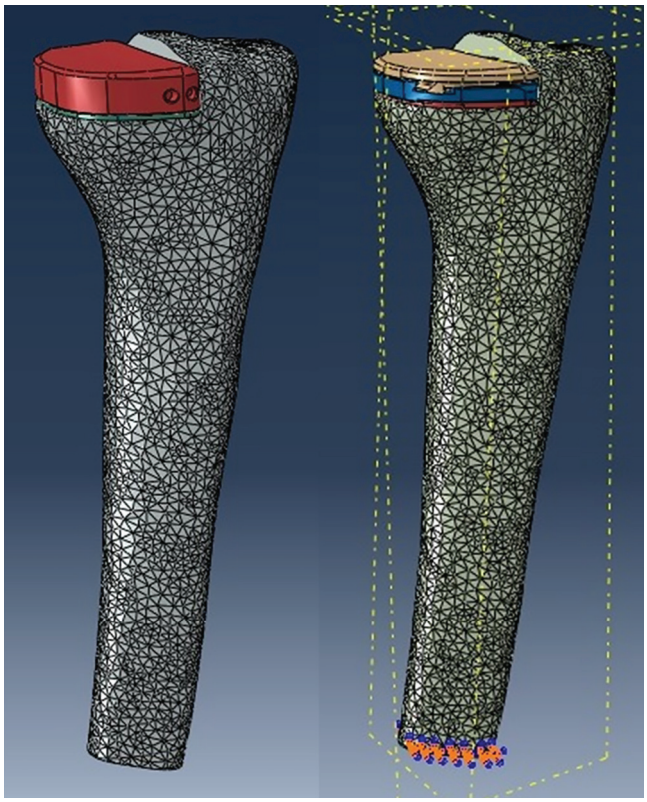

Fig. 1

FEMs with 8 mm all-polyethylene implant (left) and 8 mm metal-backed implant (right). Datum planes indicate anatomical axes used as reference for implantation.

Table I. Linear tetrahedral meshes with mean internodal distances of 1.5 mm to 2 mm were used. Mesh resolution was based on a 2% convergence criterion for the displacement magnitudes in the proximal tibia (Table I).[20,21] Cement was bonded to bone and tibial insert to metal baseplate using tie constraints. A coefficient of friction of 0.25 was used between implant and cement.[20] The distal tibia was fully constrained. Proximally, the tibia was constrained against medial/lateral and anterior/posterior translations at a node representing the anterior cruciate ligament footprint to prevent non-physiological bending.

Load was applied directly to the polyethylene articular surface. For validation purposes, the medial plateau only was loaded (this reflected the experimental setup where the aim was to detect only microdamage originating medially): distributed load, uniform weighting, applied at the central node over a radius of 6 mm (113.1 mm^2 area). This closely reflected the contact area found experimentally of 116 mm^2[15] and the contact point reported in kinematic studies.[22] A 2500 N load was applied parallel to the tibial mechanical axis. Strain data (volume of cancellous bone elements experiencing minimum principal strain $<$ -3000 με and $<$ -7000 με or maximum principal strain $>$ 3000 με and $>$ 7000 με, and peak minimum and maximum principal strains) were recorded at each 500 N increment. In accordance with the commonly used convention in engineering, the negative sign denotes compression and positive tension.

To validate each FEM against AE mechanical testing data,[15] the mean number of AE hits (sound waves of $>$ 45 dB amplitude signifying microdamage events) on loading and unloading five specimens of each implant was correlated with FEM-predicted cancellous bone strain data. DIC-measured vertical strain was correlated with FEM-predicted cortical bone vertical strain.

Statistical analysis. This was performed using SPSS version 19.0 (SPSS Inc., Chicago, Illinois). Correlation between parametric variables was assessed using Pearson's correlation coefficient. Linear regression analysis was used to explore significant correlations in continuous data with linear relationships. Autocorrelation was tested using the Durbin-Watson statistic (0, positive autocorrelation; 4, negative autocorrelation and 2, no autocorrelation) and residuals were determined to be normally distributed prior to linear regression analysis.

Additional FEM simulations. After validation, additional FEM simulations were undertaken. CAD files were manipulated to create AP tibial components and MB polyethylene inserts of 6 mm and 10 mm thicknesses by adding or removing 2 mm slices. To better represent physiological conditions, and eliminate bending from a unilateral load, a lateral plateau load was added as a distributed load at the central node with radius 6 mm. A 60:40 medial:lateral load division[23] was used and a 4170 N maximum total load (2500 N medial load) was incrementally applied. Maximum load was therefore approximately six times the

Table I. Material properties assigned to finite element model parts.[20,21] Cortical and cancellous bone properties apply to loading in compression

Model	Part	Elastic modulus (GPa)	Poisson's ratio	Elements
AP	Cortical bone	16.7	0.3	105 375
	Cancellous bone	0.155	0.3	93 880
	PMMA cement	2.4	0.3	19 691
	AP tibia	0.69	0.46	23 950
MB	Cortical bone	16.7	0.3	105 375
	Cancellous bone	0.155	0.3	96 340
	PMMA Cement	2.4	0.3	6 371
	MB tibial tray (CoCr)	210	0.3	16 594
	Polyethylene insert	0.69	0.46	22 313

AP, all-polyethylene; MB, metal-backed; GPa, gigapascal; PMMA, polymethylmethacrylate; CoCr, cobalt chrome

Table II. Pearson's correlation of acoustic emission and finite element parameters

Finite element parameter	Acoustic emission hits		
	Loading	Unloading	Total hits
Compressive strain			
Volume of elements < -3000 με	0.947*	0.942*	0.970*
Volume of elements < -7000 με	0.802	0.854*	0.831*
Tensile strain			
Volume of elements > 3000 με	0.848*	0.914*	0.881*
Volume of elements > 7000 με	0.540	0.699	0.581

*p < 0.01

patient's body weight (82 kg (804 N) mean body weight for UKA in our unit)[5] and reflects physiologic tibiofemoral loading.[24] Material properties, interactions, constraints and boundary conditions were unchanged. Numerical data were extracted for strain variables as before.

Results

FEM validation. Compressive strain correlated with AE data more closely than tensile strain (Table II). The greatest correlation existed between the volume of cancellous bone elements with compressive strain < -3000 με and the number of AE hits on loading (Table III, Fig. 2). Anteromedial cortical bone vertical strain, measured using DIC, correlated strongly with that predicted by the FEM (Pearson's correlation AP 0.956, p = 0.01; MB 0.885, p = 0.01; all implants R = 0.838, R^2 = 0.702; standard error 0.45; Durbin-Watson 0.32) (Fig. 3).

Linear regression analysis of experimental AE data and predicted FEM data are shown in Table III. Regression equations for both implants fitted the data significantly well (analysis of variance (ANOVA) p < 0.005). That is, the dependent outcome variable (AE hits on loading) was significantly predicted by the regression model using the independent FEM variables of volume of elements with strain >3000 με or < -3000 με.

For the MB implant, regression equations fitted well for all FEM variables investigated (ANOVA p < 0.01). For the AP implant, regression equations fitted well (ANOVA p < 0.05) for volume of elements with compressive strain < -3000 με. The equation for tensile strain > 3000 με did not predict AE hits significantly well (ANOVA p = 0.099). This is to be expected in a model loaded in compression.

Linear regression analysis was based on discrete AE hit data and FEM-predicted strains. The strongest correlations existed for the MB implant (Table III) (p < 0.008 *t*-test). When data for both implants were combined, correlation was greatest between AE hits and FEM-predicted volume of elements with compressive strain < -3000 με (Table III). AE-measured microdamage and FEM predicted strains were related with a confidence of > 95%.

Finite element analysis. Loading both plateaus altered the bone strain distribution for both implants: lateral strain shielding and medial metaphyseal flare strain concentrations (bending) were resolved.

Cancellous bone minimum principal strain. A greater volume of cancellous bone was strained below -3000 με and -7000 με in the 8 mm AP than the 8 mm MB model at every load (Fig. 4). At lower loads (1668 N and 2502 N), twice the volume of cancellous bone had a compressive strain of < -3000 με in the AP than in the MB implant. At 4170 N, the volume of elements with compressive strain < -7000 με was three times greater in the AP implants (Fig. 4).

Altering polyethylene thickness significantly affected the volume of overstrained cancellous bone in AP implants. At loads > 2502 N, reducing AP implant thickness from 10 mm to 6 mm increased the cancellous bone volume with compressive strain < -7000 με by 1.5 to three times (Fig. 4). Altering MB insert thickness made little difference to the volume of bone overstrained (Figs 4 and 5). AP implants displayed 2.2 (10 mm) to 3.2 (6 mm) times the volume of cancellous bone compressively overstrained < -7000 με compared with MB implants at 4170 N (Fig. 4).

Strain contours demonstrated different patterns of minimum principal strain between implants (Figs 6 to 8). In the MB implant, high compressive strain was confined to the cut tibial surface, but extended much deeper under the AP implant (Figs 6 and 7). In the AP implant, minimum principal strain was concentrated anteromedially

Table III. Linear regression analysis results of acoustic emission (AE) hits (dependent variable) against finite element model parameters (*x*: independent/predictive variables)

AE hits *vs*:	R	R^2	SE of estimate	DW	Linear regression $Y = a + bx$		SE of b	T score (p-value)	95% CI
					a	*b*			
Volume elements < -3000 με compressive									
AP	0.917	0.840	19.6	3.49	4.12	0.009	0.002	3.98 (0.028)	0.002 to 0.015
MB	0.989	0.978	3.6	2.87	6.24	0.007	0.001	11.6 (0.001)	0.005 to 0.009
All	0.947	0.847	12.6	3.3	4.27	0.008	0.001	8.37 (< 0.001)	0.006 to 0.011
Volume elements > 3000 με tensile									
AP	0.806	0.650	29.1	2.25	29.98	0.017	0.007	2.36 (0.099)	-0.006 to 0.04
MB	0.989	0.979	3.56	3.45	1.83	0.039	0.003	11.7 (0.001)	0.028 to 0.049
All	0.848	0.720	20.8	1.8	18.2	0.02	0.004	4.5 (0.002)	0.01 to 0.031

SE, standard error; DW, Durbin Watson statistic; CI, confidence interval; AP, all polyethylene; MB, metal backed

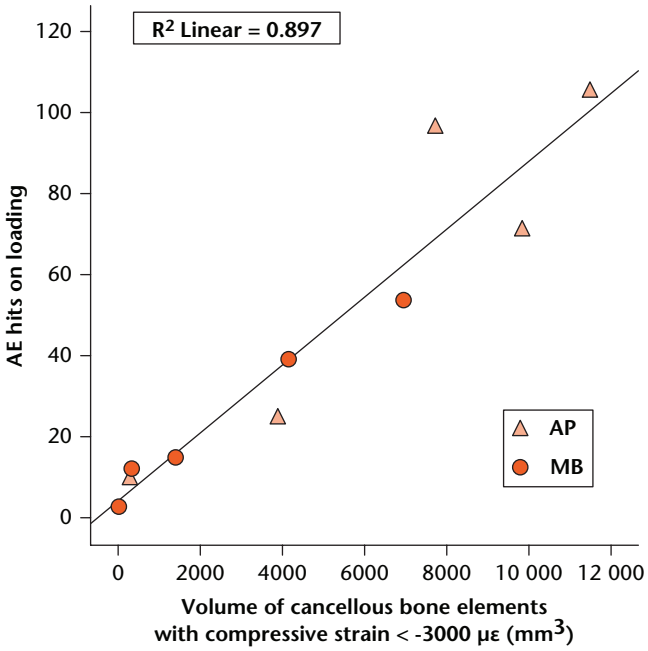

Fig. 2

Scatter graphs for both implants showing the mean number of acoustic emission (AE) hits measured at each load compared with finite element model-predicted volume of cancellous bone elements with compressive (minimum principal) strain < -3000 με (AP, all polyethylene; MB, metal backed).

in association with the keel and peg (Fig. 7), and at the posteromedial rim of the tibia (Figs 7 and 8). Reducing AP implant polyethylene thickness increased peg and keel concentrations (Fig. 8). In the MB implant, strain concentrated laterally at the implant corner and at the keel, with relative shielding at the peg (Figs 7 and 8). Altering MB insert thickness had little effect (Fig. 8). Peak minimum principal and peak maximum principal strain occurred in elements just anterior to the implant keel in both implants.

Cancellous bone maximum principal strain. When loading in compression, tensile strains are the result of Poisson's effect. Therefore, smaller volumes of cancellous bone experienced more excessive tensile than excessive compressive strains. The volume of cancellous bone with tensile strain > 3000 με differed significantly between implants at loads ⩾ 2502 N (Fig. 5). Altering MB insert thickness made little difference to the volume of overstrained bone (Fig. 5). Reducing AP thickness from 10 mm to 6 mm increased the volume of cancellous bone with tensile strain > 3000 με by 1.5 to 3.24 times at loads > 2502 N (Fig. 5). In 6 mm implants, the ratio of cancellous bone volumes with tensile strain > 3000 με (AP:MB implants) was 5.7:1 at 2502 N and 2.4:1 at 4170 N. For 10 mm implants the ratios were 2.2:1 and 1.8:1, respectively.

The volume of cancellous bone with tensile strain > 7000 με differed between implants at high loads. At 4170 N the volume of cancellous bone overstrained > 7000 με increased exponentially in the 6 mm AP

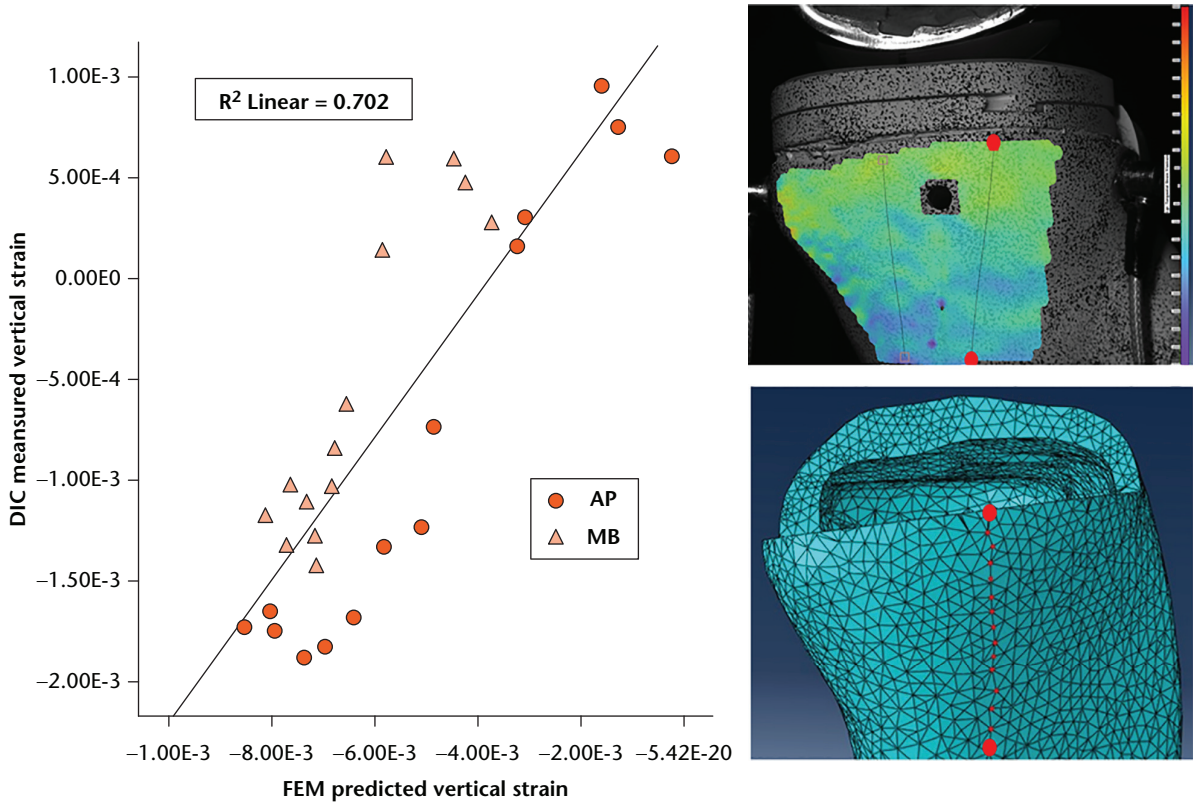

Fig. 3

Scatter graphs showing digital image correlation (DIC) measured cortical bone vertical strain along an anteromedial line for 8 mm all-polyethylene (AP) and metal-backed (MB) implants (inset) and predicted finite element model (FEM) vertical strain data at nodes along the same line (inset).

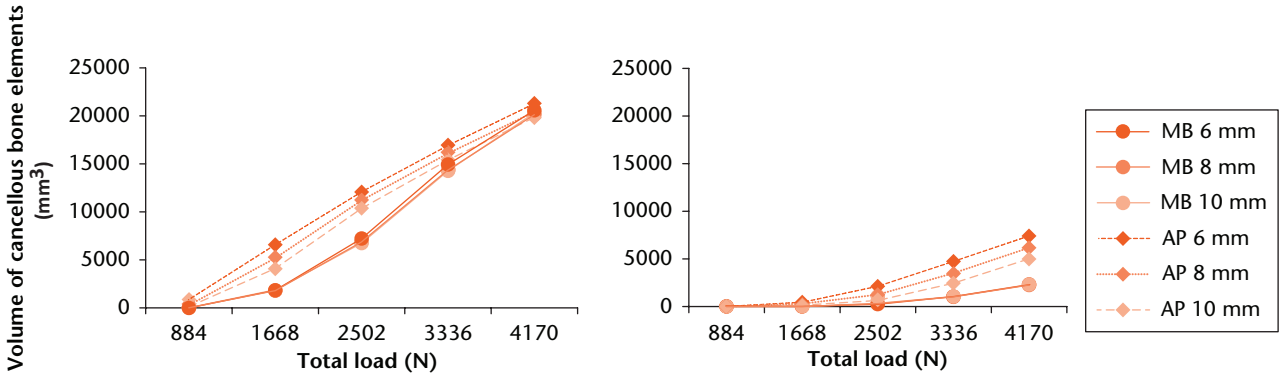

Fig. 4a Fig. 4b

Volume of cancellous bone elements with compressive (minimum principal) strain < -3000 με (a) and < -7000 με (b) for both metal-backed (MB) and all-polyethylene (AP) implants of 6 mm to 10 mm thickness.

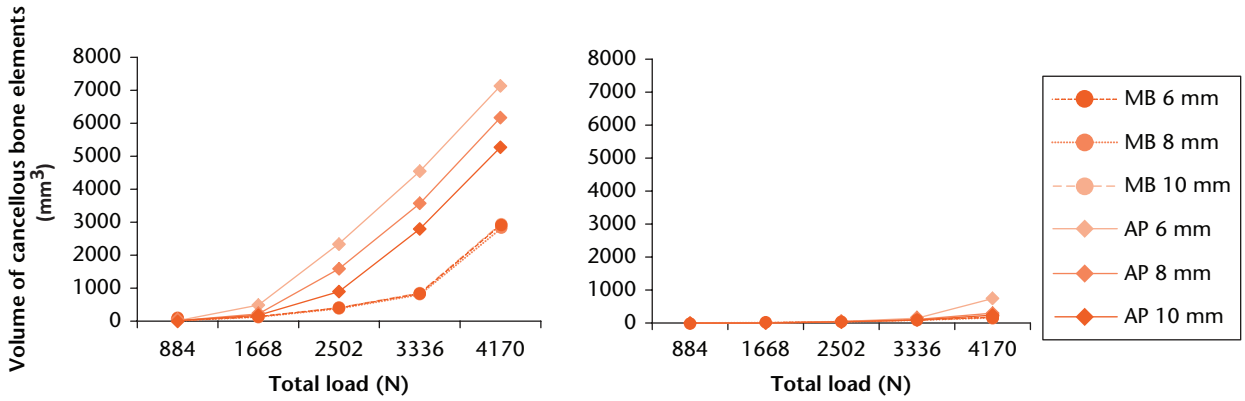

Fig. 5a Fig. 5b

Volume of cancellous bone elements with tensile strain (maximum principal strain) > 3000 με (a) and > 7000 με (b) for both metal-backed (MB) and all-polyethylene (AP) implants of 6 mm to 10 mm thickness.

implant (Fig. 5). Deformation was greater in AP implants, with more bending in both coronal and sagittal planes.

Discussion

Cancellous bone strain differed significantly between AP and MB UKA implants with greater volumes of pathologically overstrained cancellous bone in AP implants and higher peak tensile strains. This concurs with mechanical testing[15] where AP implants displayed 1.8 to six times more microdamage (AE hits) than MB implants, particularly at loads > 1000 N. Implant stiffness is a function of geometry and material properties. Large differences in the Young's moduli of polyethylene E = 0.69 GPa and cobalt-chrome E = 210 GPa[21] result in greater bending of the AP implant. Decreasing polyethylene thickness, and therefore stiffness, increased proximal tibial strain in the AP implant. Load distribution was more even in the MB implant which deformed less. The difference between implants was not overcome by increasing AP thickness to 10 mm. In MB implants, polyethyelene inserts of < 8.5 mm thickness have been associated with unacceptably high von Mises stresses,[9] but there is currently no recommended minimum polyethylene thickness for UKA. The keel-associated anteromedial strain concentration was more pronounced in the AP implant. Simpson et al[4] have reported a similar anteromedial von Mises strain concentration (140% that of an intact tibia) in the MB mobile-bearing Oxford UKA (Biomet, Swindon, United Kingdom). This has been hypothesised as a source of unexplained anteromedial pain. The lateral corner strain concentration in the MB implant has been reported previously in the Oxford implant.[4,10] This is the region with no cortical support and may reflect greater implant deformation here than at cortically supported regions.

Joint registries do not distinguish between AP and MB UKA implants. Poor survivorship of AP UKAs has been reported[25-28] with early failures commonly due to tibial loosening, subsidence or pain. Whilst ten- to 15-year survival of 90% to 92% is reported for an AP implant with minimum thickness 9 mm,[29] components of 6 mm have been associated with early clinical failure[30] and increased wear and osteolysis.[31] However, increasing AP implant thickness requires increased resection depth which reduces bone strength[32] and increases strain.[4] Thicker implants may therefore result in increased tibial component loosening or subsidence, or joint line elevation and

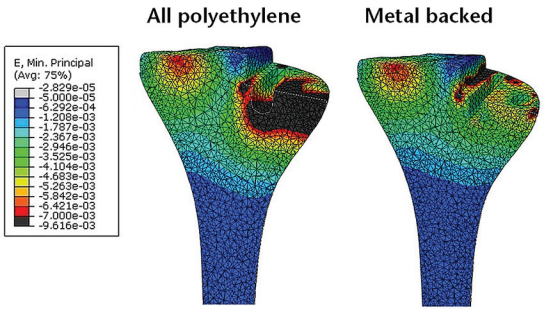

Fig. 6

Mid-coronal oblique contours of the cancellous bone for each 8 mm implant at total load of 4170 N (medial load 2500 N). Strain > -50 με appears pale grey, strain < -7000 με appears black.

coronal malalignment.[33] Increasing AP thickness must be balanced against larger bone resection. Actual minimum polyethylene thickness depends upon femoral component radius of curvature and bearing conformity: for the UKA implants here, 7.26 mm (8 mm AP implant) and 6.45 mm (8 mm MB insert).

It is argued that yielding and damage in bone is best described using strain rather than stress.[34] Strain-based criteria are numerically more efficient and accurate than stress-based criteria.[34] Previous UKA FEMs report von Mises stress and strains.[7,8,12] Gray et al[8] used 17 strain gauges to validate a composite tibia model ($R^2 = 0.962$, percentage error 5%)[8] and a cadaveric tibial model ($R^2 = 0.98$, percentage error 8.8%)[7] implanted with the Oxford UKA. Tuncer et al[11] used strain gauges to validate cadaveric tibia models with cemented ($R^2 = 0.85$) and uncemented ($R^2 = 0.62$) Oxford UKAs. Our correlation values between experimental AE data and predicted FEM data (Pearson's correlation 0.947, $R^2 = 0.847$, percentage error 12.5%) compare favourably. DIC is a recognised technique for FEM validation[16,17] and here has confirmed this validation (Pearson's correlation 0.838, $R^2 = 0.702$, percentage error 4.5%). An advantage of DIC over strain gauges in FEM validation is the number of data points produced for correlation. Grassi et al[17] used continuous field of view DIC (50 000 data points) to validate FEMs of the femur. Our experimental region of interest was limited to the proximal tibia, specifically the 30 mm beneath the implant anteromedially, a region previously demonstrated to display elevated strains in UKA.[4] Strain was measured along an anteromedial line to measure strain gradation with depth beneath the cut tibial surface instead of using whole field of view. Desite this restricted zone, > 80 data points were provided by DIC for model validation.

The threshold limits of 3000 με and 7000 με were chosen to represent the strains at which cancellous bone is pathologically overloaded and fails, respectively.[35] The volume of elements in an FEM which can experience strains above or below threshold limits (e.g. 3000 με or 7000 με) is finite. As the volume of elements experiencing high strain increases, the volume available to experience high strains declines, producing a sigmoid curve with a plateau region where further load increases cannot increase volume. This is very similar to what occurs in acoustic emission: when microfracture occurs with the emission of a hit, that region cannot emit further hits, again producing a sigmoid curve. The consequence of these sigmoid curves is non-linear relationships when

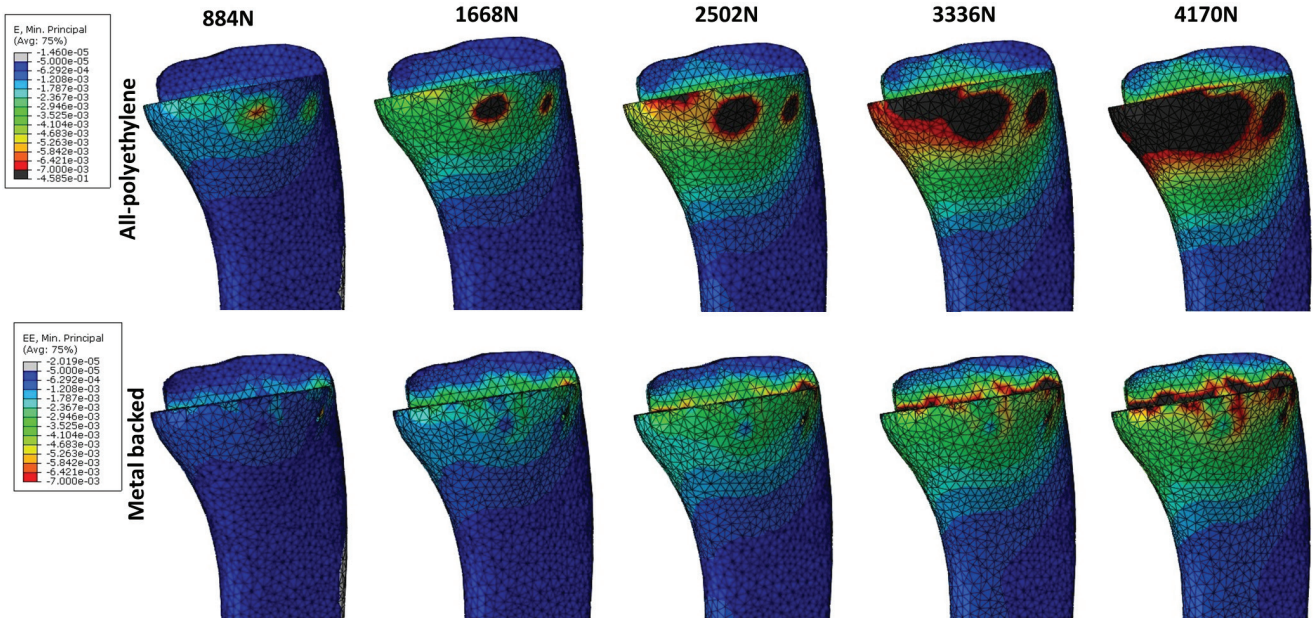

Fig. 7

Medial aspect contour of the outer surface of cancellous bone for each 8 mm implant. Strain > -50 με appears pale grey, strain < -7000 με appears black.

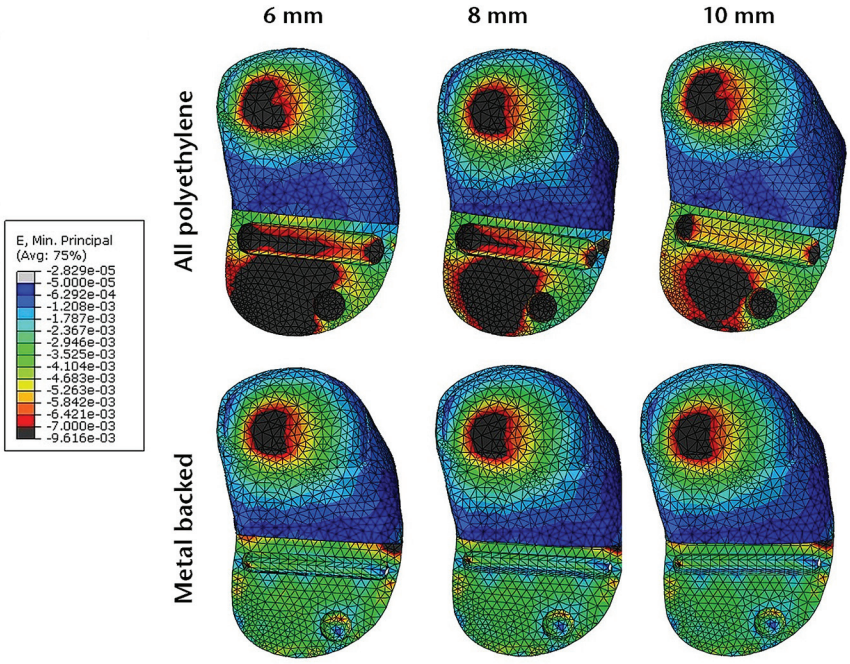

Fig. 8

Axial compressive (minimum principal) contours of the upper surface of cancellous bone for implants of different thickness at a 2502 N total load (1500 N medial load). Strain > -50 με appears pale grey, strain < -7000 με appears black.

microdamage is greatest. At lower strain thresholds (e.g. volume of elements with minimum strain < -3000 με) the graphs for AP and MB implants converge as plateaus are approached. When the threshold is increased (to < -7000 με), data shift to the linear region of the curve and differences between implants are more apparent. As MB implants remain in the linear region of the curve for the parameters measured, linear regression analyses give better predictive regression equations for MB than for AP implants.

A linear elastic FEM was used in this study. Although bone is viscoelastic with non-linear behaviour, linear modelling can be used to reduce computing requirements when loading is not cyclical and not to failure.[23,34] Our experimental data support linear model use as the Felicity effect (AE activity occurring before the previous maximum applied load is reached, indicating permanent damage) was displayed by only one specimen at the loads applied.[15]

Limitations of this study include the use of composite tibias. These do not reflect the graduated trabecular structure of proximal tibial cancellous bone, but are applicable to the "average" tibia. Fourth generation composite tibias were used experimentally whereas the FEM utilised a third generation tibia model. As the geometry did not change between these generations, only the material properties were altered, this should not have affected the results as fourth generation properties were assigned to the FE model. Anisotropic, heterogeneous bone was modelled as isotropic and homogenous and a linearly elastic analysis was performed. This is a common method and does not discredit the differences found between implants here. Gait was not modelled. As kinematic studies have shown the point of contact to change little throughout a range of movement in fixed bearing UKAs, this was considered acceptable.[22] The soft tissues of the intact lateral compartment were not modelled and this will have affected lateral strain.

This validated FEM study has shown UKAs with AP tibial components to be associated with greater proximal tibial cancellous bone strain than MB implants of the same geometry. These differences are present at physiological loads and increase at higher loads. Altering polyethylene thickness in MB implants has little effect on bone strain, but thinner polyethylene inserts display high internal strain, which may result in unfavourable wear characteristics similar to TKA.[36,37] Altering AP component thickness has marked effects on proximal tibial strain, with thinner implants associated with greater strains. Increasing AP implant thickness to 10 mm does not overcome this difference and comes at the cost of greater bone resection.

References

1. **No authors listed.** NJR of England and Wales: 12th Annual Report. http://www.njrreports.org.uk/Portals/3/PDFdownloads/NJR%2012th%20Annual%20Report%202015.pdf (date last accessed 07 December 2016).
2. **No authors listed.** Norwegian Annual Report of the Norwegian Arthroplasty Register. http://nrlweb.ihelse.net/Rapporter/Report2016_english.pdf (date last accessed 07 December 2016).
3. **No authors listed.** New Zealand Orthopaedic Association: the New Zealand Joint Registry seventeen year report. http://nzoa.org.nz/system/files/NZJR%2017%20year%20Report.pdf (date last accessed 07 December 2016).

4. **Simpson DJ, Price AJ, Gulati A, Murray DW, Gill HS.** Elevated proximal tibial strains following unicompartmental knee replacement–a possible cause of pain. *Med Eng Phys* 2009;31:752-757.
5. **Scott CE, Wade FA, Bhattacharya R, et al.** Changes in bone density in metal-backed and all-polyethylene medial unicompartmental knee arthroplasty. *J Arthroplasty* 2016;31:702-709.
6. **Small SR, Berend ME, Ritter MA, Buckley CA, Rogge RD.** Metal backing significantly decreases tibial strains in a medial unicompartmental knee arthroplasty model. *J Arthroplasty* 2011;26:777-782.
7. **Gray HA, Taddei F, Zavatsky AB, Cristofolini L, Gill HS.** Experimental validation of a finite element model of a human cadaveric tibia. *J Biomech Eng* 2008; 130:031016.
8. **Gray HA, Zavatsky AB, Taddei F, Cristofolini L, Gill HS.** Experimental validation of a finite element model of a composite tibia. *Proc Inst Mech Eng H* 2007;221:315-324.
9. **Simpson DJ, Gray H, D'Lima D, Murray DW, Gill HS.** The effect of bearing congruency, thickness and alignment on the stresses in unicompartmental knee replacements. *Clin Biomech (Bristol, Avon)* 2008;23:1148-1157.
10. **Simpson DJ, Kendrick BJ, Dodd CA, et al.** Load transfer in the proximal tibia following implantation with a unicompartmental knee replacement: a static snapshot. *Proc Inst Mech Eng H* 2011;225:521-529.
11. **Tuncer M, Cobb JP, Hansen UN, Amis AA.** Validation of multiple subject-specific finite element models of unicompartmental knee replacement. *Med Eng Phys* 2013; 35:1457-1464.
12. **Kwon OR, Kang KT, Son J, et al.** Biomechanical comparison of fixed- and mobile-bearing for unicomparmental knee arthroplasty using finite element analysis. *J Orthop Res* 2014;32:338-345.
13. **Leung SY, New AM, Browne M.** The use of complementary non-destructive evaluation methods to evaluate the integrity of the cement-bone interface. *Proc Inst Mech Eng H* 2009;223:75-86.
14. **Christen D, Levchuk A, Schori S, et al.** Deformable image registration and 3D strain mapping for the quantitative assessment of cortical bone microdamage. *J Mech Behav Biomed Mater* 2012;8:184-193.
15. **Scott CE, Eaton MJ, Nutton RW, et al.** Proximal tibial strain in medial unicompartmental knee replacements: a biomechanical study of implant design. *Bone Joint J* 2013;95-B:1339-1347.
16. **Ghosh R, Gupta S, Dickinson A, Browne M.** Experimental validation of finite element models of intact and implanted composite hemipelvises using digital image correlation. *J Biomech Eng* 2012;134:081003.
17. **Grassi L, Väänänen SP, Amin Yavari S, et al.** Experimental validation of finite element model for proximal composite femur using optical measurements. *J Mech Behav Biomed Mater* 2013;21:86-94.
18. **Cristofolini L, Viceconti M.** Mechanical validation of whole bone composite tibia models. *J Biomech* 2000;33:279–288.
19. **No authors listed.** Biomed Town. www.biomedtown.org (date last accessed 06 December 2016).
20. **Completo A, Rego A, Fonseca F, et al.** Biomechanical evaluation of proximal tibia behaviour with the use of femoral stems in revision TKA: an in vitro and finite element analysis. *Clin Biomech (Bristol, Avon)* 2010;25:159-165.
21. **Callister WD, Rethwisch DG.** *Materials Science and Engineering: An Introduction.* New York: John Wiley & Sons, Inc., 2011.
22. **Argenson JN, Komistek RD, Aubaniac JM, et al.** In vivo determination of knee kinematics for subjects implanted with a unicompartmental arthroplasty. *J Arthroplasty* 2002;17:1049-1054.
23. **Conlisk N, Howie CR, Pankaj P.** The role of complex clinical scenarios in the failure of modular components following revision total knee arthroplasty: a finite element study. *J Orthop Res* 2015;33:1134-1141.
24. **Kutzner I, Heinlein B, Graichen F, et al.** Loading of the knee joint during activities of daily living measured in vivo in five subjects. *J Biomech* 2010;43:2164-2173.
25. **Furnes O, Espehaug B, Lie SA, et al.** Failure mechanisms after unicompartmental and tricompartmental primary knee replacement with cement. *J Bone Joint Surg [Am]* 2007;89-A:519-525.
26. **Mariani EM, Bourne MH, Jackson RT, Jackson ST, Jones P.** Early failure of unicompartmental knee arthroplasty. *J Arthroplasty* 2007;22:81-84.
27. **Hamilton WG, Collier MB, Tarabee E, et al.** Incidence and reasons for reoperation after minimally invasive unicompartmental knee arthroplasty. *J Arthroplasty* 2006; 21:98-107.
28. **Bhattacharya R, Scott CE, Morris HE, Wade F, Nutton RW.** Survivorship and patient satisfaction of a fixed bearing unicompartmental knee arthroplasty incorporating an all-polyethylene tibial component. *Knee* 2012;19:348-351.
29. **Newman J, Pydisetty RV, Ackroyd C.** Unicompartmental or total knee replacement: the 15-year results of a prospective randomised controlled trial. *J Bone Joint Surg [Br]* 2009;91-B:52-57.
30. **Heck DA, Marmor L, Gibson A, Rougraff BT.** Unicompartmental knee arthroplasty. A multicenter investigation with long-term follow-up evaluation. *Clin Orthop Relat Res* 1993;286:154-159.
31. **Hernigou P, Poignard A, Filippini P, Zilber S.** Retrieved unicompartmental implants with full PE tibial components: the effects of knee alignment and polyethylene thickness on creep and wear. *Open Orthop J* 2008;2:51-56.
32. **Hvid I.** Trabecular bone strength at the knee. *Clin Orthop Relat Res* 1988;227: 210-221.
33. **Kuwashima U, Okazaki K, Tashiro Y, et al.** Correction of coronal alignment correlates with reconstruction of joint height in unicompartmental knee arthroplasty. *Bone Joint Res* 2016;4:128-133.
34. **Pankaj P, Donaldson FE.** Algorithms for a strain-based plasticity criterion for bone. *Int J Numer Method Biomed Eng* 2013;29:40-61.
35. **Frost HM.** Strain and other mechanical influences on bone strength and maintenance. *Curr Opin Orthop* 1997;8:60.
36. **Bartel DL, Bicknell VL, Wright TM.** The effect of conformity, thickness, and material on stresses in ultra-high molecular weight components for total joint replacement. *J Bone Joint Surg [Am]* 1986;68-A:1041-1051.
37. **Pijls BG, Van der Linden-Van der Zwaag HM, Nelissen RG.** Polyethylene thickness is a risk factor for wear necessitating insert exchange. *Int Orthop* 2012;36:1175-1180.

Funding Statement

- This research was supported by grants from the British Association for Surgery of the Knee (BASK), Joint Action (JA) (the orthopaedic research appeal of the British Orthopaedic Association) and the Engineering and Physical Sciences Research Council (EPSRC).

Author Contribution

- C. E. H. Scott: Concept, Physical experiments, Finite element modelling, Data collection, Data analysis, Interpretation, Manuscript preparation and revision.
- M. J. Eaton: Physical experiments, Data collection, Data analysis, Interpretation, Manuscript preparation and revision.
- R. W. Nutton: Concept, Interpretation, Manuscript preparation and revision.
- F. A. Wade: Concept, Interpretation, Manuscript preparation and revision.
- S. L. Evans: Concept, Physical experiments, Interpretation, Manuscript preparation and revision.
- P. Pankaj: Concept, Finite element modelling, Interpretation, Manuscript preparation and revision.

ICMJE Conflicts of Intrest

- M. J. Eaton declares that their institution has received funding from the Welcome Trust ISSF for a project partnered with Zimmer Biomet unrelated to this work.